

# Attomole Detection of *in Vivo* Protein Targets of Benzene in Mice

EVIDENCE FOR A HIGHLY REACTIVE METABOLITE\*

Katherine E. Williams‡§, Tonya A. Carver¶, JJ L. Miranda‡, Antti Kautiainen¶, John S. Vogel||, Karen Dingley¶, Michael A. Baldwin‡, Kenneth W. Turteltaub‡¶, and A. L. Burlingame‡\*\*‡‡

Modified proteins were detected in liver and bone marrow of mice following treatment with [<sup>14</sup>C]benzene. Stained sections were excised from one-dimensional and two-dimensional gels and converted to graphite to enable <sup>14</sup>C/<sup>13</sup>C ratios to be measured by accelerator mass spectrometry. Protein adducts of benzene or its metabolites were indicated by elevated levels of <sup>14</sup>C. A number of proteins were identified by in-gel proteolysis and conventional mass spectrometric methods with the low molecular weight proteins identified including hemoglobin and several histones. The incorporation of <sup>14</sup>C was largely proportional to the density of gel staining, giving little evidence that these proteins were specific targets for selective labeling. This was also true for individual histones subfractionated with Triton-acid-urea gels. A representative histone, H4, was isolated and digested with endopeptidase Asp-N, and the resulting peptides were separated by high performance liquid chromatography. <sup>14</sup>C levels in collected fractions were determined, and the peptides were identified by conventional mass spectrometry. The modifications were distributed throughout the protein, and no particular amino acids or groups of amino acids were identified as selective targets. Thus chemical attack by one or more benzene metabolites upon histones was identified and confirmed, but the resulting modifications appeared to be largely nonspecific. This implies high reactivity toward proteins, enabling such attack to occur at multiple sites within multiple targets. It is not known to what extent, if any, the modification of the core histones may contribute to the carcinogenicity of benzene. *Molecular & Cellular Proteomics* 1:885–895, 2002.

Human exposure to benzene occurs both occupationally in the chemical and fuel industry and environmentally through automobile exhaust, gasoline, and cigarette smoke (1). Chronic exposure to benzene is known to cause aplastic

anemia and an increased risk of acute myelogenous leukemia in humans (2, 3). High exposures result in toxic responses in rodent bone marrow, including aplastic anemia, micronuclei, leukocytopenia, and hyperplasia (4–6). Long term animal studies show that benzene causes tumors at multiple sites in mice and rats (4). However, the effects of the numerous electrophilic metabolites of benzene and molecular processes underlying hematotoxicity and leukemogenesis remain unclear.

Benzene is oxidized in the liver by cytochrome P4502E1 to form benzene oxide (7–9), which gives rise to phenol, catechol, hydroquinone, 1,2,4-benzenetriol, and ring-opened metabolites such as *trans-trans*-muconic acid (10, 11). It is the reactive metabolites of benzene that are responsible for myelotoxicity. Hydroquinone and catechol concentrate and persist in the bone marrow after benzene exposure (12, 13), and significant levels of muconic acid and glucuronide and sulfate conjugates of hydroquinone and catechol are also found (14). Hematotoxicity and leukemogenicity occur upon transport of hepatic phenolic metabolites to the various bone marrow cell populations where they are oxidized further via a peroxidase-mediated reaction to their quinone and semiquinone derivatives (15–18). Various combinations of benzene metabolites can exert a synergistic effect on multiple cellular targets leading to increased toxicity (19–21). Bone marrow is a complex tissue containing hematopoietic stem cells and stromal cells, both of which are potential targets of benzene and its metabolites. There are likely multiple cellular and molecular targets of the metabolites in the bone marrow compartment that are involved in hematotoxicity and carcinogenicity (22). Developments in the assessment of risks associated with exposure to benzene have been reviewed recently (23, 24).

Benzene is known to cause aneuploidy but is not a strong DNA binding agent and is only weakly mutagenic (25, 26). We previously determined that [<sup>14</sup>C]benzene, administered at extremely low doses in mice, bound to proteins at a higher ratio compared with DNA in the target organ, bone marrow (25, 27). Elevated levels of benzene oxide and hydroquinone adducts of hemoglobin and albumin have been observed in workers subject to benzene exposure (28, 29). It could be valuable to identify any other protein targets of benzene metabolites in the bone marrow to further our understanding of benzene-induced leukemogenesis.

From the ‡Department of Pharmaceutical Chemistry and \*\*Liver Center, University of California, San Francisco, California 94143-0446 and the ¶Biology and Biotechnology Research Program and ||Center for Accelerator Mass Spectrometry, Lawrence Livermore National Laboratory, Livermore, California 94550

Received, October 6, 2002, and in revised form, October 15, 2002  
Published, MCP Papers in Press, October 15, 2002, DOI 10.1074/mcp.M200067-MCP200

Accelerator mass spectrometry (AMS)<sup>1</sup> provides an extremely sensitive method for the detection of low level modifications of proteins (30). We have utilized this technique to develop a powerful strategy for identification of target proteins of isotopically labeled xenobiotics *in vivo*, combining AMS with high resolution two-dimensional gel electrophoresis, Triton-acid-urea gels, and HPLC to separate complex protein mixtures and biological mass spectrometry (matrix-assisted laser desorption/ionization-time-of-flight mass spectrometry (MALDI-TOF-MS) and LC-ESI-MS) to identify polypeptides bearing <sup>14</sup>C modifications. In addition to confirming previous reports of hemoglobin as a target for modification by benzene (30, 31), we also report the identification of the core histones as targets for [<sup>14</sup>C]benzene metabolites detected at attomole levels in microgram amounts of mouse bone marrow protein.

#### EXPERIMENTAL PROCEDURES

**Chemicals**—[U-<sup>14</sup>C]Benzene (specific activity, 58.2 mCi/mmol, corresponding to approximately one atom of <sup>14</sup>C per benzene molecule) was obtained from Sigma. Radiopurity was found to be >99% by HPLC. The dosing solution was prepared in filter-sterilized corn oil by dilution of the stock [<sup>14</sup>C]benzene. The dosing solution concentration was verified by liquid scintillation counting. All chemicals were analytical or electrophoresis grade and obtained from Amersham Biosciences or Sigma.

**Animals**—These investigations were conducted under established federal regulations for the care and use of laboratory animals and were approved by the Lawrence Livermore National Laboratory Animal Care Committee. Male B6C3F<sub>1</sub> mice, each weighing 22–25 g, were purchased from Charles River Laboratory and allowed to acclimate in an American Association for the Accreditation of Laboratory Animal Care (AAALAC)-accredited animal facility for a minimum of 1 week before use. Animals were housed three to a cage in filter top, polycarbonate cages with hardwood chip bedding. They were maintained on a 12-h light/dark cycle at ≈22 °C and received laboratory chow and water *ad libitum*. Each animal received a single dose of corn oil (controls) or corn oil containing [<sup>14</sup>C]benzene via intraperitoneal injection. Each dosing stock was verified by liquid scintillation counting prior to administration. Two dosage regimens were used: 155 μg/kg of body weight, sacrificed at 1.5 h post-treatment, hereafter referred to as “low dose”; and 800 μg/kg of body weight, sacrificed at 18 h post-treatment, referred to as “high dose.” All mice were euthanized by CO<sub>2</sub> asphyxiation. The 18-h time point was selected based on previous time course data (25, 27) showing maximum adduct levels in the bone marrow at this time point.

**Sample Preparation**—The humerus and femur bones were dissected from each mouse using disposable scalpels and forceps (those from the control mice being collected first) to ensure no <sup>14</sup>C cross-contamination occurred. Tissues were not perfused to remove residual blood. The marrow was flushed from the bone shaft with 2 ml of phosphate-buffered saline, pH 7.4 using a disposable 26-gauge needle. Bone marrow from each treatment group was pooled, and the

cells were washed three times in phosphate-buffered saline and centrifuged at 1000 × *g*. Cells were lysed in 9 M urea, 4% CHAPS, 65 mM dithiothreitol, 2% ampholytes (Pharmalyte 3–10), 10 mM spermine, 40 mM Tris base and then centrifuged at 450,000 × *g* for 10 min at 22 °C in a Beckman TL100 tabletop ultracentrifuge to remove DNA. Protein concentrations in the supernatants were determined by a modified Bradford assay (31) using the Bio-Rad protein assay kit and ovalbumin as a standard. Samples were stored at –80 °C prior to electrophoresis. Livers were dissected, cut into small pieces, and washed twice in 20 mM Tris-HCl, pH 7.4. The tissue was homogenized in 3 volumes of the same buffer and centrifuged at 9000 × *g* for 20 min. The supernatant was lysed with 2 volumes of sample buffer (2% SDS, 10% glycerol, 5% β-mercaptoethanol, 0.025% bromphenol blue), boiled for 5 min, and stored at –20 °C for at least 30 min. For histone purification, the acid-soluble histone fraction of bone marrow was precipitated with acetone (32, 33) and dissolved in H<sub>2</sub>O.

**One-dimensional Electrophoresis**—Proteins were separated on 15% polyacrylamide gels and stained with 1% Coomassie Brilliant Blue in 50% methanol, 10% acetic acid. Triton-acetic acid-urea (TAU) gels (15% acrylamide) were run according to Waterborg (34). Densitometry was carried out using ImageMaster (Amersham Biosciences).

**Two-dimensional Electrophoresis**—Bone marrow proteins (100 μg) were separated by non-equilibrating pH gradient gel electrophoresis (35) in 15-cm rod gels containing carrier ampholytes (pH 3–10) for 2400 V-h. The gels were equilibrated for 10 min in 2% SDS, 5% dithiothreitol, 10% glycerol, trace bromphenol blue, and 1.5% Tris-HCl, pH 6.8 (36) prior to SDS-PAGE in 15% polyacrylamide gels. Proteins were visualized by silver staining (37). Four identical two-dimensional gels were run for the <sup>14</sup>C-containing bone marrow, and four gels were run for the controls. Each of the labeled gels and three unlabeled gels were analyzed separately by AMS. A fourth control gel was used for in-gel digestion, peptide extraction, and identification by MALDI-MS and LC-ESI-MS.

**HPLC**—Reversed phase HPLC was performed on a Beckman Gold system. Core histones were separated based on previously published methods (32, 33) using a 180-μm × 15-cm C4 column (Vydac) and eluted with a 38–55% B linear gradient over 120 min (Buffer A: 0.1% heptafluorobutyric acid in H<sub>2</sub>O; buffer B, 0.08% heptafluorobutyric acid in acetonitrile). HPLC separation of AspN-digested peptides of histone H4 was carried out using a C18 column (180 μm × 15 cm) (LC Packings, San Francisco, CA) with an Applied Biosystems 140B syringe pump.

**AMS**—Disposable materials were used for any item that might come in contact with a sample to prevent cross-contamination between samples. Gel spots were excised with disposable plastic drinking straws and placed in 6- × 50-mm quartz tubes. Tributyrin was added as a carrier to HPLC fractions. Samples were dried by vacuum centrifugation, and the dried samples were reduced to graphite using published protocols (38). For [<sup>14</sup>C]benzene analysis, we measured <sup>14</sup>C relative to <sup>13</sup>C and normalized to the ratio of 1950 AD carbon using the Australian National University sugar reference standard (39). The carbon contents of the samples was determined using a C:N:S analyzer (Carlo-Erba NA1500, series 2). Hemoglobin was determined to have a carbon content of 50.38%.

**Enzymatic Digestion of Proteins**—The procedure of Clauser *et al.* (40) was used with minor modifications for the tryptic digestion of proteins in polyacrylamide gels. Each spot was excised, diced, and vortexed three times for 10 min in 50% acetonitrile, 25 mM ammonium bicarbonate. The gel pieces were dried in a Speedvac, resuspended in 25 mM ammonium bicarbonate with 12.5 ng/μl trypsin, and digested overnight at 37 °C. The peptides were extracted by vortexing three times for 10 min in 50% acetonitrile, 5% trifluoroacetic acid. Extracts were pooled, concentrated in a Speedvac to ~1–2 μl, and dissolved in 10 μl of 50% acetonitrile, 5% trifluoroacetic acid. HPLC-

<sup>1</sup> The abbreviations used are: AMS, accelerator mass spectrometry; HPLC, high performance liquid chromatography; MALDI, matrix-assisted laser desorption/ionization; TOF, time-of-flight; MS, mass spectrometry; LC, liquid chromatography; ESI, electrospray ionization; CHAPS, 3-[(3-cholamidopropyl)dimethylammonio]-1-propanesulfonic acid; TAU, Triton-acetic acid-urea.

separated histone H4 was digested with AspN for 4 h in 50 mM sodium phosphate, pH 8.0 at 37 °C.

**Mass Spectrometry**—The molecular masses of peptides were determined by analyzing the unseparated tryptic digests using one of three mass spectrometric techniques. Routine peptide analysis utilized a MALDI-TOF DE STR mass spectrometer (Applied Biosystems, Framingham, MA) operated in reflectron mode. One-tenth of each sample digest was mixed in a 1:1 ratio with 33 mM  $\alpha$ -cyano-4-hydroxycinnamic acid solution (Agilent, Palo Alto, CA). Spectra were internally calibrated using known trypsin autolysis products (41). Selected ions were subjected to postsource decay analysis (42, 43). High energy positive ion collision-induced dissociation mass spectra were acquired on a Kratos Analytical Instruments Concept IIHH four-sector tandem mass spectrometer (Kratos, Manchester, UK) (44) equipped with a continuous flow, liquid inlet probe for liquid secondary ionization and a scanning charge-coupled device array detector. For HPLC-MS, a capillary HPLC system (ABI, Foster City, CA) was interfaced directly to a Mariner orthogonal acceleration time-of-flight mass spectrometer using electrospray ionization (Applied Biosystems). The unseparated digests were diluted in water and injected directly into a 180- $\mu$ m  $\times$  15-cm capillary C18 column (LC Packings). Online HPLC-MS was performed using a formic acid/ethanol/propylol solvent system (45) with a gradient of 5–60% solvent B in 2 h. A cone voltage setting of 175 V was used for collision-induced dissociation, giving rise to fragment ion peaks. Peptide masses and fragment ion masses measured by either MALDI-MS or LC-ESI-MS were analyzed with the MS-Fit and MS-Tag programs in ProteinProspector (prospector.ucsf.edu) (46). Mass accuracy in both MALDI-MS (internally calibrated) and ESI-MS was generally 50 ppm or better.

## RESULTS

**Identificaton of  $^{14}\text{C}$  in Proteins from SDS-PAGE**—AMS was used to determine the  $^{14}\text{C}$  incorporation in proteins separated by one-dimensional SDS-PAGE with Coomassie Blue staining throughout the molecular mass range up to 120 kDa in liver (low dose only) and bone marrow (low dose and high dose). In the liver, the highest levels of the heavy isotope were found in the protein fraction corresponding to the molecular mass range of 45–55 kDa (Fig. 1, upper panel). By contrast, in bone marrow the distribution of  $^{14}\text{C}$  proteins for both low and high dose showed the highest levels of incorporation in a band of 12–15 kDa. The distribution of  $^{14}\text{C}$  throughout the molecular mass range was similar for both doses of benzene in the bone marrow. It was noted that all regions of the gels showed significant levels of isotope incorporation compared with naturally occurring levels in undosed controls, suggesting that at least a substantial fraction of this incorporation was nonspecific. We performed similar gel analysis on fractions enriched for cytosolic, nuclear, and microsomal proteins from exposed liver and bone marrow to obtain subcellular localization for protein targets of benzene metabolites. The highest levels of incorporation in the liver were found in microsomes and cytosol, whereas the bone marrow showed  $^{14}\text{C}$  enrichment in the nuclei (data not shown).

The protein fractions containing the highest heavy isotope levels corresponding to 45–55 kDa from liver and 12–15 kDa from bone marrow were subjected to in-gel trypsin digestion. The extracted peptides were separated by HPLC, their molecular masses were determined by MALDI-MS, and in some

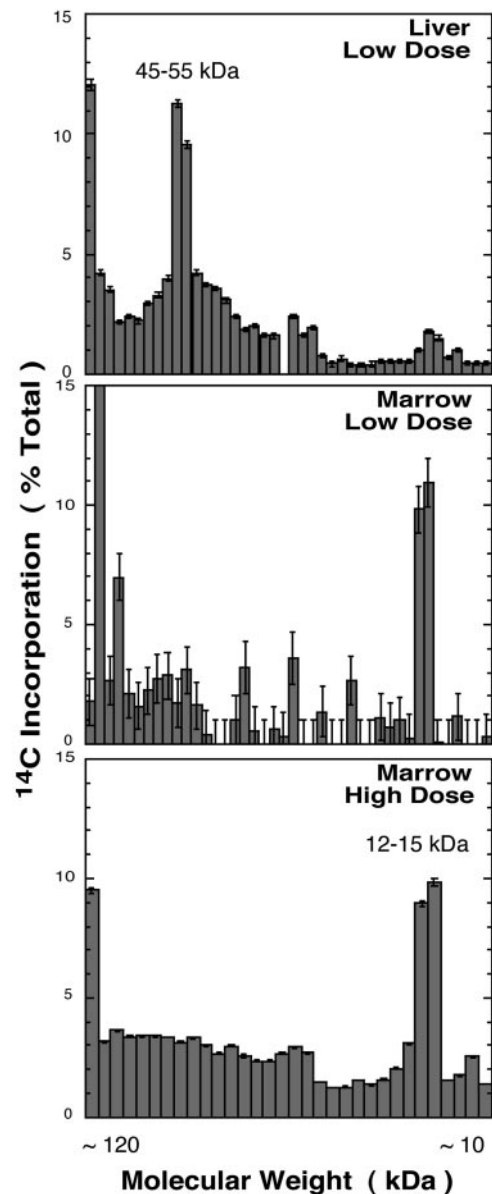


Fig. 1.  $^{14}\text{C}$  content in gel slices cut from SDS-PAGE-separated proteins from liver (low dose) and bone marrow (low dose and high dose). Each gel lane was divided into sections and submitted for AMS analysis. The data are expressed as the percentage of total  $^{14}\text{C}$  incorporation across each gel lane after subtraction of controls. For the upper two panels the controls were sections of gel between the lanes. For the lower panel the control was a gel lane run with protein from untreated mice. The left-hand side of each panel represents the top of the gel, containing proteins that did not enter the gel, typically of molecular mass >120 kDa. The right-hand side represents the dye front with proteins <10 kDa.

cases they were identified by tandem mass spectrometry using high energy collision-induced dissociation. Five different polypeptides were identified in the 45–55-kDa liver fraction: the  $\alpha$  and  $\beta$  chains of ATP synthase, disulfide isomerase, aldehyde dehydrogenase, and elongation factor EF-1  $\alpha$ -chain (Table I). In the 12–15-kDa bone marrow fraction, we identified

TABLE I  
Protein identification from one-dimensional gel slices using in-gel digestion and high energy CID of peptides

Sample source	Identity (NCBI no.)	Obtained sequences	Matching sequences
Liver			
~15 kDa	Chaperonin 10 (2493662)	FLPLFDR (Q/K)FLPLFDR	(K)FLPLFDR(V) (R)KFLPLFDR(V)
~55 kDa	ATP synthase a-subunit (416677)	APGIIPR ELIIGDR VLSIGDGIAR AVDS(I/L)VPIGR	(K)APGIIPR(I) (R)ELIIGDR(Q) (R)VLSIGDGIAR(V) (K)AVDSLVPPIGR(G)
	ATP synthase a-subunit (3023356)	VALTGLTVAEYFR (I/L)GLFGGAGVGK	(R)VALTGLTVAEYFR(D) (K)IGLFGGAGVGK(T)
	Elongation factor 1-a (72870)	(Q/K)TVAVGVK	(R)QTVAVGVK(A)
	Disulfide isomerase (68462)	(I/L)LEFFG(I/L)K THILLFLPK	(R)ILEFFGLK(K) (K)THILLFLPK(S)
	Aldehyde dehydrogenase (1352250)	AAF(Q/K)LGSPWR (I/L)LYR	(R)AAFQLGSPWR(R) (R)LLYR(L)
Bone marrow			
~10–15 kDa	Histone H2B (2119001)	(I/L)AHYNKR	(R)LAHYNKR(S)
	Histone H3 (122075)	(I/L)LLPGELAK (Q/K)LPF(Q/R)R	(R)LLLPGELAK(H) (R)KLPFQR(L)
	Histone H2A (121961)	HL(Q/K)LAIR AGL(Q/K)FPVGR	(R)HLQLAIR(N)
	$\alpha$ -Hemoglobin (122441)	MFASFPTTK SA(Q/K)VK	(R)MFASFPTTK(T) (G)SAQVK(G)
	$\beta$ -Hemoglobin (122513)	(I/L)(I/L)VV	(R)LLVV(Y)
~15–20 kDa	Histone H2A (121961)	HL(Q/K)LAIR AGL(Q/K)FPVGR	(R)HLQLAIR(N) (R)AGLQFPVGR(V)
~55 kDa	Actin (809561)	DLTDYLMK (I/L)IAPPER	(R)DLTDYLMK(I) (K)IAPPER(K)

$\alpha$ - and  $\beta$ -hemoglobin and the core histones H2A, H2B, and H3 as unresolved components. Histones H2A, H2B, and H3 were also identified from the 12–15-kDa region of bone marrow fractions enriched for nuclear proteins.

The amount of  $^{14}\text{C}$  in each region of the gels was compared with relative protein abundances as determined by densitometry. It was noted that the profiles for isotope incorporation along the gel bands were very similar to the densitometer profiles, e.g. see the densitometer and  $^{14}\text{C}$  profiles for bone marrow (high dose) depleted in red blood cells (Fig. 2). This observation that  $^{14}\text{C}$  levels are proportional to protein concentration, independent of protein molecular mass, suggests that a large part of protein adduct formation is a nonspecific effect that is independent of the nature of the proteins.

*Identification of  $^{14}\text{C}$  in Proteins from Two-dimensional Gels*—As histones had been identified in the one-dimensional gel slices with elevated  $^{14}\text{C}$  levels and as histones are central to the structure and function of chromatin, we surmised that molecular damage to histone proteins might be capable of producing the cellular abnormalities observed in benzene toxicity. It was desired to establish whether histones were indeed a target for benzene metabolite modification. Because the histone and hemoglobin signals were coincident in the same one-dimensional slices, we were concerned that higher levels

of enrichment in low level proteins could be masked by more abundant species, therefore two-dimensional separation was carried out. Histone proteins have basic isoelectric points in the range of 10–11.5; consequently the cellular homogenate was separated in the first dimension using non-equilibrating pH gradient gel electrophoresis, which is optimal for the separation of basic polypeptides (32). Four control gels of protein from mice not treated with benzene were prepared in an identical manner, one of which is shown in Fig. 3. Focusing primarily on the 12–15-kDa molecular mass and basic pI range, selected spots were excised for AMS (four treated and three untreated gels) or conventional mass spectrometry (one untreated gel). Other more intensely stained spots corresponding to proteins of higher molecular mass were also taken for analysis.

The gel spots intended for conventional mass spectrometry were subjected to in-gel digestion and identification by MALDI-MS and/or LC-ESI-MS, the results of which are summarized in Table II. The most strongly stained spots, 21 and 22, were found to include both  $\alpha$ - and  $\beta$ -hemoglobin. Spots 30 and 31 at ~30 kDa also gave peptide masses matching both  $\alpha$ - and  $\beta$ -hemoglobin, most likely due to hemoglobin dimers. Spots 27 and 28 in the ~10-kDa region of the gel also contained  $\alpha$ - and  $\beta$ -hemoglobin, N-terminal and C-terminal peptides being seen for both isoforms. As these do not ap-

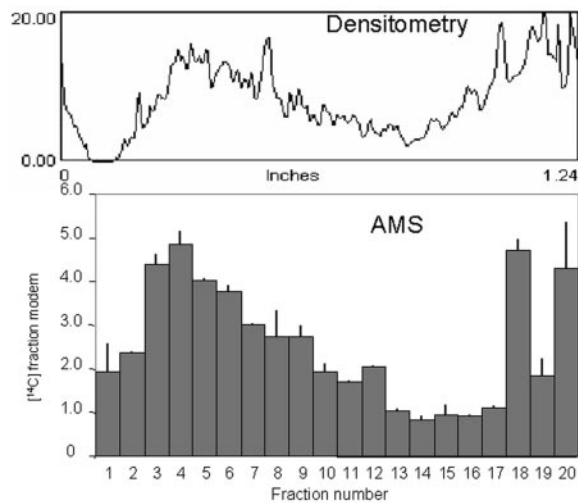


FIG. 2. Comparison of the density of staining (top) and the  $^{14}\text{C}$  content (bottom) in slices from a one-dimensional gel used to separate bone marrow proteins (high dose) depleted in red blood cells. Error bars represent the uncertainty in the AMS measurements. The left-hand side represents the top of the gel.

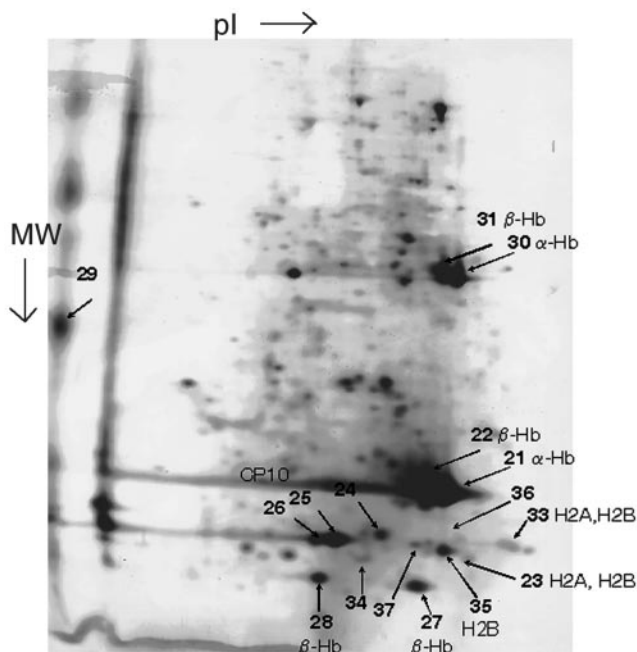


FIG. 3. One of four silver-stained two-dimensional gels from electrophoresis of protein homogenates from bone marrow extracted from untreated mice. Four identical gels were prepared from bone marrow extracted from mice treated with benzene (high dose). The numbered spots were cut from all the treated gels and three of the untreated gels and subjected to  $^{14}\text{C}$  analysis by AMS. Equivalent spots from the remaining untreated gel were used for protein identification by conventional mass spectrometry.

pear to be truncated forms of the protein, their presence in this region of the gel is surprising and unexplained. Of the remaining highly basic spots in the  $\sim 12$ – $14$ -kDa region, 23 and 33 were identified as containing a mixture of histone H2A

and histone H2B, whereas spot 35 was identified to contain only histone H2B. Spot 25 was identified as the murine cytokine CP-10, the peptides giving 87% sequence coverage. No identifications could be made for spectra from in-gel digests of spots 24, 34, 36, and 37.

The AMS measurements shown in Fig. 4 for the excised gel spots demonstrate that the strongly stained spots 21 and 22 contained the bulk of the isotopic label, and the weakly stained histone spots showed only low levels of incorporation. Silver staining is not ideal for quantitation, particularly with the wide dynamic range of proteins represented by these gels, and the basic histones are known to stain poorly with silver. Therefore from this experiment it was not possible to accurately compare the relative amounts of incorporation of  $^{14}\text{C}$  into the histones per unit of protein. However, compared with hemoglobin, these data gave no indication of any low level proteins being significantly more enriched in  $^{14}\text{C}$ .

*Analysis of Core Histones for AMS Analysis*—The foregoing experiments suggested that the histones were not necessarily specific targets for higher than average incorporation of benzene metabolites. However, not all the histones had been identified by the two-dimensional gel separation. Therefore, in a separate experiment, core histones were purified from the bone marrow of mice receiving the high dose of [ $^{14}\text{C}$ ]benzene. The histones were separated on one-dimensional TAU gels and stained with Coomassie Brilliant Blue, which would give more quantitative staining. The heavy isotope content was determined by AMS, and the proteins in each band were identified by trypsin digestion and MALDI mass spectrometry. Fig. 5 shows one lane from a TAU gel, the histones identified within each band, and the  $^{14}\text{C}$  content of each band as determined by AMS. The wide dynamic range for the stained bands that were identified as containing histones is reflected in the widely varying  $^{14}\text{C}$  content. However, when the AMS results were normalized based on the protein abundances as quantitated by densitometry, all identified histones, H1, H2A, H2B, H3, and H4, contained the same amount of the isotopic label per unit of protein within  $\pm 30\%$ . This experiment clearly shows that the degree of  $^{14}\text{C}$  incorporation is independent of the specific histone, and no histones stand out as being particularly susceptible to covalent modification by benzene or its metabolites.

*HPLC Purification of Histone H4 Peptides for Adduct Localization*—A representative histone was chosen for further study to determine whether or not the covalent modification by benzene metabolites was associated with specific amino acids or sites within the protein. HPLC-purified histone H4 from the high dose experiment was digested in solution using endoproteinase AspN, the peptides were separated by HPLC, and fractions were collected (Fig. 6, upper panel). One-tenth of each fraction was analyzed by conventional mass spectrometry to identify the peptides (Table III), and the remainder of each fraction was analyzed for  $^{14}\text{C}$  content by AMS as shown by the gray bars in the lower panel of Fig. 6. Full

## Protein Targets for Benzene Metabolites Using AMS

TABLE II  
Proteins identified in spots cut from the two-dimensional gel (Fig. 3)

Due to the polymorphism of  $\beta$ -hemoglobin in mouse, several variants were found. Each peptide is marked as belonging to one of the following variants: s (single), j (D major), or n (D minor).

Spot no.	Identity (NCBI no.)	Observed mass	Sequence
21	$\alpha$ -Hemoglobin (122441)	1529.73	(K)IGGHGAEYGAEALER(M)
		1029.51	(R)MFASFPPTK(T)
		1819.89	(K)TYFPHFVDVSHGSAQVK(G)
		1087.62	(K)LRVDPVNFK(L)
		1571.77	(K)FLASVSTVLTSKYR(-)
22	$\beta$ -Hemoglobin (122513)	912.50	(M)VHLTDAEK(A) <sup>s,j,n</sup>
		888.53	(K)AAVSGLWGK(V) <sup>s</sup>
		1005.55	(K)AAVSCLWGK(V) <sup>j</sup>
		1035.56	(K)SAVSCLWAK(V) <sup>n</sup>
		1286.65	(K)VNADEVGGEALGR(L) <sup>s</sup>
		1302.64	(K)VNSDEVGGEALGR(L) <sup>j</sup>
		1312.67	(K)VNPDEVGGEALGR(L) <sup>n</sup>
		1274.74	(R)LLVYPWTQR(Y) <sup>s,j,n</sup>
		1980.92	(R)YFSSFGLSSADAIMGNAK(V) <sup>s,j</sup>
		2006.95	(R)YFDSFGLSSASAIMGNPK(V) <sup>n</sup>
		1756.97	(K)VITAFSDGLNHLNLDNLK(G) <sup>s,j</sup>
		1091.65	(K)VITAFNEGLK(N) <sup>n</sup>
		716.41	(K)NLDNLK(G) <sup>n</sup>
		1478.71	(K)GTFASLSELHCDK(L) <sup>s,j,n</sup>
		1126.60	(K)LHVDPENFR(L) <sup>s,j,n</sup>
		1714.09	(R)LLGNMIVIVLGHHLGK(D) <sup>s,j</sup>
		1654.09	(R)LLGNAIVIVLGHHLGK(D) <sup>n</sup>
1294.66	(K)DFTPAQAQAFQK(V) <sup>s,j,n</sup>		
1106.69	(K)VVAGVAAALAHK(Y) <sup>s</sup>		
1136.71	(K)VVAGVATALAHK(Y) <sup>j,n</sup>		
23	Histone H2A (121961)	733.39	(K)QGCKAR(A)
		944.52	(R)AGLQFPVGR(V)
		1441.77	(Y)LTAEILELAGNAAR(D)
		850.52	(R)HLQLAIR(N)
		1931.05	(R)VTIAQGGVLPNIQAVLLPK(K)
	Histone H2B (2119001)	1168.57	(K)QVHPDTGISSK(A)
		1743.75	(K)AMGIMNSFVNDIFER(I)
		733.39	(R)IASEASR(L)
		901.50	(R)LAHYNKR(S)
		664.37	(R)STITSR(E)
		816.46	(R)EIQTAVR(L)
25, 26	CP-10 (1173338)	953.59	(R)LLLPGELAK(H)
		828.43	(K)HAVSEGTK(A)
		833.42	(-)MPSELEK(A)
		2784.38	(K)ALSNLIDVYHNSNIQGNHHALYK(N)
		3416.69	(K)ALSNLIDVYHNSNIQGNHHALYKNDFFK(M)
27	$\beta$ -Hemoglobin (122513)	2467.19	(K)MVTTECPQFVQNIENLFR(E)
		2425.20	(R)ELDINSDNAINFEEFLAMVIK(V)
		912.47	(M)VHLTDAEK(A) <sup>s,j,n</sup>
		888.49	(K)AAVSGLWGK(V) <sup>s</sup>
		1005.51	(K)AAVSCLWGK(V) <sup>j</sup>
		1035.54	(K)SAVSCLWAK(V) <sup>n</sup>
		1286.60	(K)VNADEVGGEALGR(L) <sup>s</sup>
		1302.59	(K)VNSDEVGGEALGR(L) <sup>j</sup>
		1312.64	(K)VNPDEVGGEALGR(L) <sup>n</sup>
		1274.69	(R)LLVYPWTQR(Y) <sup>s,j,n</sup>
1980.85	(R)YFSSFGLSSADAIMGNAK(V) <sup>s,j</sup>		
2006.89	(R)YFDSFGLSSASAIMGNPK(V) <sup>n</sup>		
1478.67	(K)GTFASLSELHCDK(L) <sup>s,j,n</sup>		
1126.56	(K)LHVDPENFR(L) <sup>s,j,n</sup>		
1714.02	(R)LLGNMIVIVLGHHLGK(D) <sup>s,j</sup>		
1654.02	(R)LLGNAIVIVLGHHLGK(D) <sup>n</sup>		

TABLE II—continued

Spot no.	Identity (NCBI no.)	Observed mass	Sequence
28	$\beta$ -Hemoglobin (122513)	1294.64	(K)DFTPAAQAAFQK(V) <sup>s,j,n</sup>
		1106.67	(K)VVAGVAAALAHK(Y) <sup>s</sup>
		1136.67	(K)VVAGVATALAHK(Y) <sup>j,n</sup>
		912.50	(M)VHLTDAEK(A) <sup>s,j,n</sup>
		888.52	(K)AAVSGLWGK(V) <sup>s</sup>
		1005.55	(K)AAVSCLWGK(V) <sup>j</sup>
		1035.56	(K)SAVSCLWAK(V) <sup>n</sup>
		1286.67	(K)VNADEVGGEALGR(L) <sup>s</sup>
		1302.66	(K)VNSDEVGGEALGR(L) <sup>j</sup>
		1312.69	(K)VNPDEVGGEALGR(L) <sup>n</sup>
		1274.75	(R)LLVVYPWQR(Y) <sup>s,j,n</sup>
		1980.95	(R)YFSSFGDLSSADAIMGNAK(V) <sup>s,j</sup>
		2006.98	(R)YFDSFGDLSSASAIMGNPK(V) <sup>n</sup>
		1756.97	(K)VITAFSDGLNHLNLDNLK(G) <sup>s,j</sup>
		1091.64	(K)VITAFNEGLK(N) <sup>n</sup>
		1478.72	(K)GTFASLSELHCDK(L) <sup>s,j,n</sup>
		1126.59	(K)LHVDPENFR(L) <sup>s,j,n</sup>
1714.08	(R)LLGNMIVIVLGHHLGK(D) <sup>s,j</sup>		
1654.07	(R)LLGNAIVIVLGHHLGK(D) <sup>n</sup>		
1294.68	(K)DFTPAAQAAFQK(V) <sup>s,j,n</sup>		
1106.71	(K)VVAGVAAALAHK(Y) <sup>s</sup>		
1136.71	(K)VVAGVATALAHK(Y) <sup>j,n</sup>		
31	$\alpha$ -Hemoglobin (122441)	1529.80	(K)IGGHGAEYGAALER(M)
		1029.53	(R)MFASFPTTK(T)
		1820.01	(K)TYFPHFDVSHGSAQVK(G)
		1087.65	(K)LRVDPVNFK(L)
		1571.86	(K)FLASVSTVLTSKYR(-)
33	Histone H2A (121961)	733.39	(K)QGCKAR(A)
		944.54	(R)AGLQFPVGR(V)
		1441.80	(Y)LTAEILELAGNAAR(D)
		850.53	(R)HLQLAIR(N)
		1931.17	(R)VTIAQGGVLPNIQAVLLPK(K)
	Histone H2B (2119001)	1168.59	(K)QVHPDTGISSK(A)
		1743.81	(K)AMGIMNSFVNDIFER(I)
		733.39	(R)IASEASR(L)
		901.50	(R)LAHYNKR(S)
		664.38	(R)STITSR(E)
35	Histone 2B (2119001)	816.46	(R)EIQTAVR(L)
		953.60	(R)LLPGELAK(H)
		828.43	(K)HAVSEGTK(A)
		1168.63	(K)QVHPDTGISSK(A)
		1743.90	(K)AMGIMNSFVNDIFER(I)
		816.49	(R)EIQTAVR(L)
		953.64	(R)LLPGELAK(H)

coverage of the protein sequence was not obtained; some fractions were found to contain multiple peptides, and no peptides were identified in the later fractions. Although the levels of  $^{14}\text{C}$  determined by AMS showed wide variation across the various fractions, when the level of  $^{14}\text{C}$  incorporation was normalized to the area of the HPLC peaks, which for absorption at 214 nm should be approximately proportional to the product of peptide concentration and the number of amino acids per peptide, all HPLC fractions showed significant incorporation of the label, and there were no obvious peptides that were strongly favored for modification as shown by the *black bars* in Fig. 6.

## DISCUSSION

In this study we detected and measured covalent protein modifications by  $^{14}\text{C}$ -containing metabolites of benzene in the bone marrow of mice. This approach allowed us to measure attomole levels of isotope, in this case  $^{14}\text{C}$ , in individual proteins at levels of one adduct per  $10^6$  protein molecules. For  $\beta$ -hemoglobin (spot 22), we calculated an adduct level less than 1 fmol/ $\mu\text{g}$ . Using gas chromatography/mass spectrometry, hemoglobin had previously been identified as a target for modification by benzene metabolites (28, 29). However, the methodology developed here is applicable to the more general identification and characterization of proteins modified by

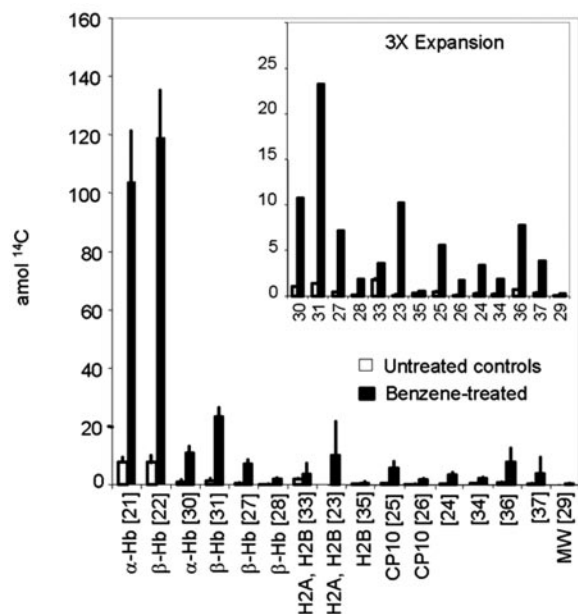


FIG. 4. Mean incorporation of <sup>14</sup>C in bone marrow proteins in spots cut from the two-dimensional gels. Error bars show standard deviations from four experiments using benzene-treated mice (solid bars) and three using untreated controls (open bars). The inset shows a 3× expanded view of all but the two strongest signals.

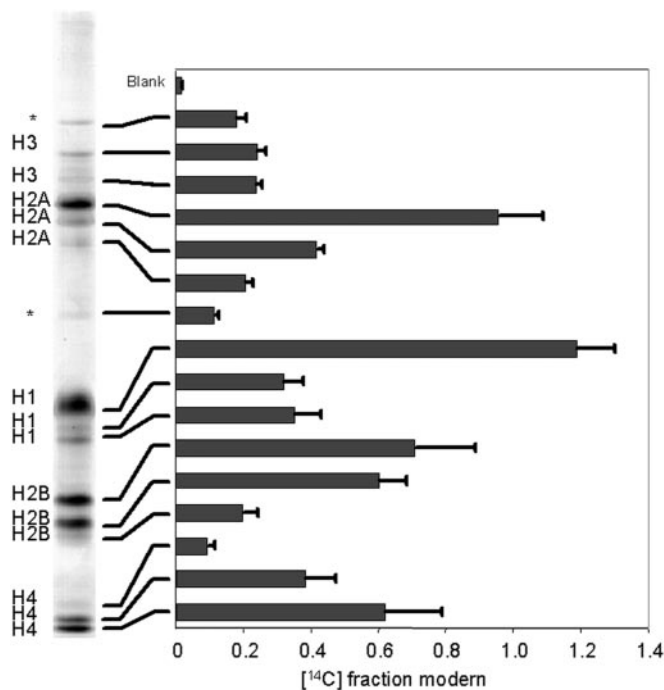


FIG. 5. Incorporation of <sup>14</sup>C in core histones separated using TAU gels. Left, TAU gel with histones identified by MALDI; bands labeled \* were not identified. Right, <sup>14</sup>C incorporation measured by AMS, expressed as fraction modern (38).

xenobiotics *in vivo* at very low exposure levels and using small amounts of protein without prior knowledge of the structural nature of the adduct.

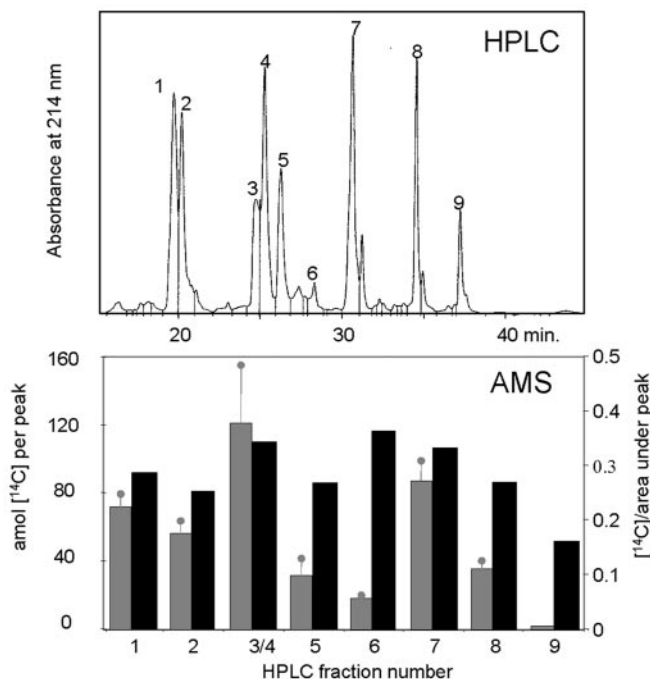


FIG. 6. Analysis of histone H4 digested with AspN after isolation from bone marrow (high dose). Top, reversed phase HPLC of peptides, monitored by UV absorption at 214 nm, showing fractions collected for peptide identification by conventional mass spectrometry (10% of each fraction) and measurement of <sup>14</sup>C by AMS (90%). Bottom, gray bars show the amount of <sup>14</sup>C detected in each fraction by AMS; black bars show the same quantity divided by the area of the corresponding HPLC peak (arbitrary units).

We note that a limitation of the AMS approach using <sup>14</sup>C as a tracer is that it can only detect the presence of carbon-containing adducts. The methods adopted here would not detect other covalent changes arising from processes such as oxidation or hydrolysis of the targets.

The profile of <sup>14</sup>C distributed across the one-dimensional gel slices revealed a differential distribution in the liver and bone marrow. However, the protein distributions for these samples were also different, and proteins identified in the same molecular mass range in the bone marrow and in the liver were not all the same. Hemoglobin was identified only in the 12–15-kDa bone marrow gel slice and not in the liver gel slice in the same molecular mass range. There could be numerous proteins in that molecular mass range of a one-dimensional gel slice, and it is likely that only a subset of these would be identified by mass spectrometry. Subcellular fractionation prior to one-dimensional analysis improved the dynamic range and simplified the identification of <sup>14</sup>C-labeled proteins but still did not allow definitive identification of individual protein targets for modification.

To correlate heavy isotope incorporation with individual polypeptides, we used the high resolving power of two-dimensional electrophoresis to separate the components of the 12–15-kDa bone marrow band prior to AMS. The isotope label

TABLE III

Peptides identified in the AspN digest of histone H4 based on mass analysis and PSD

Note that several peptides resulted from nonspecific cleavages.

SGRGKGGKGLGKGGAKRHRKVLR DNIQGITKPAIRRLARRGGVKRISGLIYEETR  
GVLKVFLENVIR DAVTYTEHAKRKTVTAM DVYALKRQGRTLYGFGG

HPLC fraction no.	Peptides identified
1	SGRGKGGKGLGKGGAKRHRKVL, LENVIR, VYALKRQGR <u>TLY</u>
2	LENVIR, VYALKRQGR <u>TLY</u>
3 + 4	ALKRQGR <u>TLYG</u> FGG
5	FLENVIR, RISGLIYEET, DNIQGITKPAIRRL
6	GVLKVFLENVIR, DNIQGITKPAIRRL
7	ALKRQGR <u>TLYG</u> FGG, YALKRQGR <u>TLY</u>
8, 9	No peptides identified

in the 12–15-kDa band of the bone marrow was partitioned primarily into the nuclear compartment, and we focused on the molecular mass and pI range in two-dimensional gels that would incorporate the histones to identify benzene adducts. The use of two-dimensional electrophoresis significantly improved the dynamic range over one-dimensional gels, and the use of in-gel digestion and mass spectrometric analysis permitted rapid identification of the proteins of interest from the two-dimensional gels. The majority of the label in the protein homogenates from bone marrow proved to be associated with hemoglobin. This likely resulted from peripheral blood in the bone marrow preparation. For future studies, contaminating mature red blood cells could be removed from bone marrow samples by suspending the sample in a hypotonic solution to lyse the red blood cells prior to homogenization (47).

The one-dimensional gel analysis suggested that histones might be targets for attack by benzene or its metabolites. This was confirmed by two-dimensional separation, although silver staining did not allow the quantitation of the modified species. However, subsequent enrichment of the histones and one-dimensional separation by TAU gels with more quantitative Coomassie Blue staining gave no indication that any specific histone was a favored target for modification. This is despite the fact that the amino acid compositions of the various histones vary quite widely. For example histone H2A contains one cysteine residue that might be a target for modification, whereas H2B contains no cysteine residues. All histones are lysine-rich, and the nucleophilic  $\epsilon$ -amino group of lysine may also be a binding site for benzene metabolites. Few peptides derived by digestion of H4 contain no lysine residues, and every HPLC fraction was found to contain at least one peptide that included at least one lysine residue. Thus the observation that all HPLC fractions gave similar  $^{14}\text{C}$  levels when normalized to the area of their UV peaks at 214 nm suggests that their susceptibility to modification by reactive benzene metabolites could be due to the presence of lysine, although it should be noted that alanine, arginine, glycine, isoleucine, leucine, threonine, and tyrosine were also represented in at least one peptide within each fraction.

The findings reported here demonstrate that benzene me-

tabolites are highly reactive and appear relatively promiscuous in their selection of protein targets. Detailed investigation of the histones demonstrates that their attack by reactive benzene species is ubiquitous, resulting in multiple modified sites within a single histone. Of the amino acids potentially susceptible to reaction, cysteine is not an exclusive target, whereas lysine could be. The evidence suggests that multiple lysine residues within each histone are attacked, the location of each modification being based on rates of diffusion rather than kinetic factors. This highly reactive nature of the benzene metabolites suggests a free radical mechanism. A number of authors have presented evidence for free radical mechanisms in benzene toxicity as reviewed by Subrahmanyam *et al.* (17). As free radicals the metabolites would have short half-lives, therefore protein targets for attack would need to be closely associated with a region in which benzene or its less reactive metabolites might accumulate after environmental or occupational exposure. Accumulation in the bone marrow cells could place the substrate for formation of reactive species close to chromatin, thereby allowing histone modification to proceed relatively efficiently. Accumulation in red blood cells would also contribute to the modifications seen in hemoglobin.

The modification of histone proteins by the known leukemogenic agent benzene is intriguing in light of the role of histones in transcription and chromosome structure and function. Acetylation of the highly conserved lysine residues in the N-terminal tails of the core histones results in chromatin structural changes and gene expression (48–51). Lysine acetylation reduces inhibition of transcription, and abnormal acetylation/deacetylation can lead to cancer development (52). A number of histone deacetylase inhibitors are under investigation as novel anticancer drugs (53). Histone methylation has also been known for a long time, and it is now realized that, like acetylation, methylation also plays an important role in biological regulation (54). We have recently described analytical methods that greatly increase the sensitivity with which specific sites of both acetylation and methylation can be identified in histones (55, 56). The acetylated histones have a lower affinity for chromatin and may be more accessible to modification. The turnover of histones is low (57), so the effects of modification by

benzene metabolites could be stable and could yet prove to play a role in the process of carcinogenesis.

In earlier work on the identification of the hepatic protein targets of acetaminophen and a non-toxic regioisomer, we were able to use conventional tandem mass spectrometry not only to identify the major proteins but also to characterize the nature and sites of modification (58, 59). In the current study, any further structural analysis subsequent to AMS was hampered by small sample sizes and low stoichiometry, resulting from the apparently indiscriminate modification of a wide range of targets. Because there proved to be many proteins over a wide range of molecular masses susceptible to benzene modification, we could not identify the chemical structures of the reactive metabolites of benzene or the particular sites of modification. To achieve this it will be necessary to maximize the sensitivity of other mass spectrometric techniques to provide further information about the molecular changes associated with benzene exposure, including the site-specific structural characterization of the histone modifications indicated by the AMS analysis. Hopefully the identification of the structures of protein adducts would also identify the reactive species responsible and could indicate the metabolic pathways that are most important in benzene carcinogenicity.

In identifying histones as targets for benzene modification, this study validates a new method for identifying molecular modifications that will impact future biological studies. AMS detection of  $^{14}\text{C}$ , being up to  $10^6$ -fold more sensitive than scintillation counting (60), allowed us to localize isotopically labeled adducts in one-dimensional and two-dimensional gel separations of proteins from mice exposed to low doses of [ $^{14}\text{C}$ ]benzene with attomole sensitivity. Proteins were then identified by established mass spectrometric methods. In the future this combination of high sensitivity detection of protein modification and high resolution separation and protein identification can be applied to study a wide range of trace toxic, carcinogenic, and therapeutic compounds at physiologically relevant levels and to monitor biological events occurring with low frequency.

*Acknowledgments*—We gratefully acknowledge F. Nilsson, K. Haach, V. Laiko, C. Mani, and K. Curtis for technical assistance and S. P. H. T. Freeman and B. A. Buchholz for operation of the accelerator mass spectrometer.

\* This work was supported by University of California Systemwide Campus-Laboratory Consortium (to A. L. B.), National Center for Research Resources (NCRR) Grant RR13461 (to K. W. T.), NCRR Grant RR01614 (to A. L. B.), and Liver Center Grant DK26743 (to A. L. B.). The costs of publication of this article were defrayed in part by the payment of page charges. This article must therefore be hereby marked "advertisement" in accordance with 18 U.S.C. Section 1734 solely to indicate this fact.

§ Current address: Comprehensive Cancer Center, University of California, San Francisco, CA 94143-0808.

‡‡ To whom correspondence should be addressed: Dept. of Pharmaceutical Chemistry, University of California, San Francisco, Box

0448, 521 Parnassus Ave., San Francisco, CA 94143-0446. Tel.: 415-476-5641; Fax: 415-476-0688; E-mail: alb@itsa.ucsf.edu.

#### REFERENCES

- Wallace, L. A. (1989) The exposure of the general population to benzene. *Environ. Health Perspect.* **82**, 165–169
- Goldstein, B. D. J. (1977) Benzene toxicity: a critical evaluation: introduction. *Toxicol. Environ. Health* **2**, (suppl.) 69–105
- Rinsky, R. A., Smith, A. B., Hornung, R. F., Filloon, T. G., Young, R. J., Okun, A. H., and Landrigan, P. J. (1987) Benzene and leukemia. An epidemiologic risk assessment. *N. Engl. J. Med.* **316**, 1044–1050
- Huff, J. E., Haseman, J. K., DeMarini, D. M., Eustis, S., Maronpot, R. R., Peters, A. C., Pershing, R. L., Chrisp, C. C., and Jacobs, A. C. (1989) Multiple-site carcinogenicity of benzene in Fischer 344 rats and B6C3F1 mice. *Environ. Health Perspect.* **82**, 125–163
- Snyder, C. A., Goldstein, B. D., Sellakumar, A., Wolman, S. R., Bromberg, I., Erlichman, M. N., and Laskin, S. (1978) Hematotoxicity of inhaled benzene to Sprague-Dawley rats and AKR mice at 300 ppm. *J. Toxicol. Environ. Health* **4**, 605–619
- MacEachern, L., Snyder, R., and Laskin, D. L. (1992) Alterations in the morphology and functional activity of bone marrow phagocytes following benzene treatment of mice. *Toxicol. Appl. Pharmacol.* **117**, 147–154
- Snyder, R., Witz, G., and Goldstein, B. D. (1993) The toxicology of benzene. *Environ. Health Perspect.* **100**, 293–306
- Kalf, G. F. (1987) Recent advances in the metabolism and toxicity of benzene. *CRC Crit. Rev. Toxicol.* **18**, 141–159
- Lovern, M. R., Turner, M. J., Meyer, M., Kedderis, G. L., Bechtold, W. E., and Schlosser, P. M. (1997) Identification of benzene oxide as a product of benzene metabolism by mouse, rat, and human liver microsomes. *Carcinogenesis* **18**, 1695–1700
- Cooper, K. R., and Snyder, R. (1988) in *Benzene Carcinogenicity* (Askoy, M., ed) pp. 33–58, CRC Press, Boca Raton, FL
- Seaton, M. J., Schlosser, P. M., Bond, J. A., and Medinsky, M. A. (1994) Benzene metabolism by human liver microsomes in relation to cytochrome P450 2E1 activity. *Carcinogenesis* **15**, 1799–1806
- Rickert, D. E., Baker, T. S., Bus, J. S., Barrow, C. S., and Irons, R. D. (1979) Benzene disposition in the rat after exposure by inhalation. *Toxicol. Appl. Pharmacol.* **49**, 417–423
- Rickert, D. E., Baker, T. S., and Chism, J. P. (1981) Analytical approaches to the study of the disposition of myelotoxic agents. *Environ. Health Perspect.* **39**, 5–10
- Sabourin, P. J., Bechtold, W. E., Birnbaum, L. S., Lucier, G., and Henderson, R. F. (1988) Differences in the metabolism and disposition of inhaled [ $^3\text{H}$ ]benzene by F344/N rats and B6C3F1 mice. *Toxicol. Appl. Pharmacol.* **94**, 128–140
- Kalf, G., Shurina, R., Renz, J., and Schlosser, M. (1991) The role of hepatic metabolites of benzene in bone marrow peroxidase-mediated myeloid and genotoxicity. *Adv. Exp. Med. Biol.* **283**, 443–455
- Sadler, A., Subrahmanyam, V. V., and Ross, D. (1988) Oxidation of catechol by horseradish peroxidase and human leukocyte peroxidase: reactions of o-benzoquinone and o-benzosemiquinone. *Toxicol. Appl. Pharmacol.* **93**, 62–71
- Subrahmanyam, V. V., Ross, D., Eastmond, D. A., and Smith, M. T. (1991) Potential role of free radicals in benzene-induced myelotoxicity and leukemia. *Free Radic. Biol. Med.* **11**, 495–515
- Smith, M. T., Yager, J. W., Steinmetz, K., and Eastmond, D. A. (1989) Peroxidase-dependent metabolism of benzene's phenolic metabolites and its potential role in benzene toxicity and carcinogenicity. *Environ. Health Perspect.* **82**, 23–29
- Eastmond, D. A., Smith, M. T., and Irons, R. D. (1987) An interaction of benzene metabolites reproduces the myelotoxicity observed with benzene exposure. *Toxicol. Appl. Pharmacol.* **91**, 85–95
- Barale, R., Marrazzini, A., Betti, C., Vangelisti, V., Loprieno, N., and Barrai, I. (1990) Genotoxicity of two metabolites of benzene: phenol and hydroquinone show strong synergistic effects in vivo. *Mutat. Res.* **244**, 15–20
- Guy, R. L., Hu, P., Witz, G., and Goldstein, B. D. (1991) Depression of iron uptake into erythrocytes in mice by treatment with the combined benzene metabolites p-benzoquinone, muconaldehyde and hydroquinone. *J. Appl. Toxicol.* **11**, 443–446
- Ross, D. (1996) Metabolic basis of benzene toxicity. *Eur. J. Haematol. Suppl.* **60**, 111–118

23. Zeise, L., and McDonald, T. A. (2000) California perspective on the assessment of benzene toxicological risks. *J. Toxicol. Environ. Health Part A* **61**, 479–483
24. Kacew, S., and Lemaire, I. (2000) Recent developments in benzene risk assessment. *J. Toxicol. Environ. Health Part A* **61**, 485–498
25. Creek, M. R., Mani, C., Vogel, J. S., and Turteltaub, K. W. (1997) Tissue distribution and macromolecular binding of extremely low doses of [<sup>14</sup>C]-benzene in B6C3F1 mice. *Carcinogenesis* **18**, 2421–2427
26. Dean, B. J. (1985) Recent findings on the genetic toxicology of benzene, toluene, xylenes and phenols. *Mutat. Res.* **154**, 153–181
27. Mani, C., Freeman, S., Nelson, D. O., Vogel, J. S., and Turteltaub, K. W. (1999) Species and strain comparisons in the macromolecular binding of extremely low doses of [<sup>14</sup>C]benzene in rodents, using accelerator mass spectrometry. *Toxicol. Appl. Pharmacol.* **159**, 83–90
28. Yeowell-O'Connell, K., Rothman, N., Smith M. T., Hayes, R. B., Li, G., Waidyanatha, S., Dosemeci, M., Zhang, L., Yin, S., Titenko-Holland, N., and Rappaport, S. M. (1998) Hemoglobin and albumin adducts of benzene oxide among workers exposed to high levels of benzene. *Carcinogenesis* **19**, 1565–1571
29. Yeowell-O'Connell, K., Rothman, N., Waidyanatha, S., Smith, M. T., Hayes, R. B., Li, G., Bechtold, W. E., Dosemeci, M., Zhang, L., Yin, S., and Rappaport, S. M. (2001) Protein adducts of 1,4-benzoquinone and benzene oxide among smokers and nonsmokers exposed to benzene in China. *Cancer Epidemiol. Biomark. Prev.* **10**, 831–838
30. Vogel, J. S., Grant, P. B., Buchholz, B. A., Dingley, K., and Turteltaub, K. W. (2001) Attomole quantitation of protein separations with accelerator mass spectrometry. *Electrophoresis* **22**, 2037–2045
31. Ramagli, L. S., and Rodriguez, L. V. (1985) Quantifying protein in 2-D PAGE solubilization buffers. *Electrophoresis* **6**, 559–563
32. Yoshida, M., Kijima, M., Akita, M., and Beppu, T. (1990) Potent and specific inhibition of mammalian histone deacetylase both *in vivo* and *in vitro* by trichostatin A. *J. Biol. Chem.* **265**, 17174–17179
33. Cousens, L. S., Gallwitz, D., and Alberts, B. M. (1979) Different accessibilities in chromatin to histone acetylase. *J. Biol. Chem.* **254**, 1716–1723
34. Waterborg, J. H. (1996) in *The Protein Protocols Handbook* (Walker, J. M., ed) pp. 91–100, Humana Press, Totowa, NJ
35. O'Farrell, P. Z., Goodman, H. M., and O'Farrell, P. H. (1977) High resolution two-dimensional electrophoresis of basic as well as acidic proteins. *Cell* **12**, 1133–1141
36. O'Farrell, P. H. (1975) High resolution two-dimensional electrophoresis of proteins. *J. Biol. Chem.* **250**, 4007–4021
37. Shevchenko, A., Wilm, M., Vorm, O., and Mann, M. (1996) Mass spectrometric sequencing of proteins silver-stained polyacrylamide gels. *Anal. Chem.* **68**, 850–858
38. Vogel, J. S. (1992) Rapid production of graphite without contamination for biomedical AMS. *Radiocarbon* **3**, 344–350
39. Turteltaub, K. W., and Vogel, J. S. (1996) in *Mass Spectrometry in the Biological Sciences* (Burlingame, A. L., and Carr, S. A., eds) pp. 477–495, Humana Press, Totowa, NJ
40. Clauser, K. R., Hall S. C., Smith, D. M., Webb, J. W., Andrews, L. E., Tran, H. M., Epstein, L. B., and Burlingame, A. L. (1995) Rapid mass spectrometric sequencing and peptide mass matching for characterization of human melanoma proteins isolated by two-dimensional PAGE. *Proc. Natl. Acad. Sci. U. S. A.* **92**, 5072–5076
41. Vestling, M. M., Murphy, C. M., and Fenselau, C. (1990) Recognition of trypsin autolysis products by high-performance liquid chromatography and mass spectrometry. *Anal. Chem.* **62**, 2391–2394
42. Spengler, B., Kirsch, D., Kaufmann, R., and Jaeger, E. (1992) Peptide sequencing by matrix-assisted laser-desorption mass spectrometry. *Rapid Commun. Mass Spectrom.* **6**, 105–108
43. Yu, W., Vath, J. E., Huberty, M. C., and Martin, S. A. (1993) Identification of the facile gas-phase cleavage of the Asp-Pro and Asp-Xxx peptide bonds in matrix-assisted laser desorption time-of-flight mass spectrometry. *Anal. Chem.* **65**, 3015–3023
44. Walls, F. C., Baldwin, M. A., Falick, A. M., Gibson, B. W., Kaur, S., Maltby, D. A., Gillece-Castro, B. L., Medzihradsky, K. F., Evans, S., and Burlingame, A. L. (1990) in *Biological Mass Spectrometry* (Burlingame, A. L., and McCloskey, J. A., eds) pp. 285–314, Elsevier, New York
45. Feldhoff, R. (1991) in *Techniques in Protein Chemistry II* (Villafranca, J. J., ed) pp. 55–63, Academic Press, Inc., San Diego, CA
46. Clauser, K. R., Baker, P., and Burlingame, A. L. (1996) in *Proceedings of the 44th ASMS Conference on Mass Spectrometry and Allied Topics, Portland, OR, May 12–16, 1996*, p. 365, American Society for Mass Spectrometry, Santa Fe, NM
47. Subrahmanyam, V., Sadler, A., Suba, E., and Ross, D. (1989) Stimulation of *in vitro* bioactivation of hydroquinone by phenol in bone marrow cells. *Drug Metab. Dispos.* **17**, 348–350
48. Hassig, C. A., and Schreiber, S. L. (1997) Nuclear histone acetylases and deacetylases and transcriptional regulation: HATs off to HDACs. *Curr. Opin. Cell Biol.* **1**, 300–308
49. Wade, P. A., and Wolffe, A. P. (1997) Histone acetyltransferases in control. *Curr. Biol.* **7**, 82–84
50. Grunstein, M. (1997) Histone acetylation in chromatin structure and transcription. *Nature* **389**, 349–352
51. Roth, S. Y., Denu, J. M., and Allis, C. D. (2001) Histone acetyltransferases. *Annu. Rev. Biochem.* **70**, 81–120
52. Lin, R. J., Nagy, L., Inoue, S., Shao, W., Miller, W. H., and Evans, R. M. (1998) Role of the histone deacetylase complex in acute promyelocytic leukaemia. *Nature* **391**, 811–814
53. Marks, P. A., Richon, V. M., Breslow, R., and Rifkind, R. A. (2001) Histone deacetylase inhibitors as new cancer drugs. *Curr. Opin. Oncol.* **13**, 477–483
54. Rice, J. C., and Allis, C. D. (2001) Histone methylation versus histone acetylation: new insights into epigenetic regulation. *Curr. Opin. Cell Biol.* **13**, 263–273
55. Zhang, K., Tang, H., Huang, L., Blankenship, J. W., Jones, P. R., Xiang, F., Yau, P. M., and Burlingame, A. L. (2002) Identification of acetylation and methylation sites of histone H3 from chicken erythrocytes by high-accuracy matrix-assisted laser desorption ionization-time-of-flight, matrix-assisted laser desorption ionization-postsource decay, and nano-electrospray ionization mass spectrometry. *Anal. Biochem.* **306**, 259–269
56. Zhang, K., Williams, K. E., Huang, L., Yau, P. M., Siino, J. S., Bradbury, E. M., Jones, P. R., Minch, M. J., and Burlingame, A. L. (2002) Histone acetylation and deacetylation: identification of acetylation sites of HeLa histone H4 by mass spectrometry. *Mol. Cell. Proteomics* **1**, 500–508
57. Allfrey, V. G., and Boffa, L. C. (1979) in *The Cell Nucleus* (Busch, H., ed) Vol. 7, pp. 521–562, Academic Press, New York
58. Qiu, Y., Benet, L. Z., and Burlingame, A. L. (1998) Identification of the hepatic protein targets of reactive metabolites of acetaminophen *in vivo* in mouse using 2-D gel electrophoresis and mass spectrometry. *J. Biol. Chem.* **273**, 17940–17953
59. Qiu, Y., Benet, L. Z., and Burlingame, A. L. (2001) in *Biological Reactive Intermediates VI: Chemical and Biological Mechanisms in Susceptibility to and Prevention of Environmental Diseases* (Dansette, P., Snyder, R., Delaforge, M., Gibson, G. G., Greim, H., Jollow, D., Monks, T., and Sipes, I., eds) pp. 663–673, Kluwer Academic/Plenum, New York
60. Vogel, J. S., Turteltaub, K. W., Felton, J. S., Gledhill B. L., Nelson, D. E., Southon J. R., Proctor, I. D., and Davis, J. C. (1990) Application of AMS to the biomedical sciences. *Nucl. Instrum. Methods Phys. Res. B* **52**, 524–530